Electric-field-induced resonances of highly excited molecules

Yasuyuki Kimura*

Quantum Dot Research Center, National Institute for Materials Science, 3-13 Sakura, Tsukuba 305-0003, Japan

(Received 4 February 2008; revised manuscript received 30 January 2009; published 15 April 2009)

In an electric field of 0–6.67 kV/cm, nitric oxide (NO) molecules are excited by the double-resonance technique through the intermediate $A\ ^2\Sigma^+F_1(v=0,N=0)$ level to the high Rydberg electronic states converging to the ionic $NO^+X\ ^1\Sigma^+(v^+=0,N^+=0)$ level, in the energy region from the classical field-ionization limit $E_C^{(0,0)}$ to above the zero-field-ionization limit $E_0^{(0,0)}$. Just below $E_0^{(0,0)}$, resonances showing Fano profiles through the field-induced autoionization are observed. Above $E_0^{(0,0)}$, resonances corresponding to the transient states of electrons trapped on the "uphill" side of the potential energy raised by the field are observed. These field-induced resonances of molecules from the negative energy region just below the zero-field-ionization limit $E_0^{(0,0)}$ to the positive energy region are assigned completely. Decoupling of the orbital angular momentum of the Rydberg electron from the core rotation is confirmed in a high electric field.

DOI: 10.1103/PhysRevA.79.043412 PACS number(s): 33.80.Eh, 32.60.+i, 33.80.Rv

I. INTRODUCTION

Effects of a high electric field on structures and dynamics of atoms and molecules have evoked continuing interest for a long time. High Rydberg states are the ideal states for observing nonperturbative effects induced by a high electric field because the field (F) of several kV/cm competes with or dominates the Coulomb binding field for a Rydberg electron when it stays far from a core, and the external field changes the shape of the Coulomb potential energy to have a saddle point (classical field-ionization limit $E_C=E_0-2\sqrt{F}$) below the zero-field-ionization limit E_0. For a hydrogen atom, even in a high field, wave functions are separable in parabolic coordinates, $\xi=r+z$ and $\eta=r-z$, where r is the radius of the electron and z is its component along the field. The n manifold is split into Stark levels denoted by parabolic quantum numbers n_1 and n_2 in the field, where n is the principal quantum number [1,2]. Potential energy in the η coordinate has a saddle point. Its energy, and thus the threshold energy for the field ionization, i.e., the parabolic critical energy E_P, is different for each Stark level and for m_l, where m_l denotes the quantum number associated with the projection along the field of the orbital angular momentum of the electron $\boldsymbol{l}$ [2,3]. The high Rydberg states of a nonhydrogenic atom in a field can be approximated by these hydrogenic states because the electron stays far from the core for most of the time. However, when it approaches the core, the non-Coulomb part of the core potential couples the Stark levels of different n_1 (core coupling). When a discrete level of high n_1 is coupled to a continuum of low n_1 lies above its E_P, the electron autoionizes [2,4]. This process is known as field-induced autoionization. A lot of experiments have been reported on these field-induced resonances [5,6], and Fano profiles have been clearly observed [7].

Above E_0, where all the n_1 channels were open, however, resonances were also observed in Rb atoms, and they were explained to be induced by electrons transiently trapped on the "uphill" side of the potential energy raised by the external field [3,8]. Few groups succeeded in observing these resonances with positive energy, where one-electron atoms such as alkali-metal atoms (Rb and Na) [9,10] or hydrogen atoms [11,12] were used, except one experiment (Ba) [10]. Theoretical explanations were presented based on both semiclassical [13] and quantum-mechanical calculations [14]. To date, on the field-induced resonances of atoms, a lot of theoretical studies [15–17] have been constantly reported for both the positive and negative (below E_0) energy regions. A lot of experimental studies have also been constantly reported [18–21] following the above-mentioned experiments, but they have been limited to the negative energy region.

For molecules, however, remarkably little was known about the Stark effect and thus about field-induced resonances in high Rydberg states. This was a result of an experimental difficulty caused by the high density of the high Rydberg states converging to the different rovibrational states of the ionic core. Resonances in an electric field were first observed in vibrationally and rotationally excited Na_2 molecules. However, the decay process was not identified as being the field-induced autoionization because the vibrational autoionization or the rotational autoionization were competing with it [22]. By using molecules in the lowest vibrational and rotational core state, field-induced resonances could be observed being distinguished from resonances caused by these competing processes. Around the classical field-ionization limit, these experiments were performed only for H_2 molecules in a field of 5 kV/cm, where resonances were assigned by the fourth-order perturbation theory [23], and for NO molecules below 1 kV/cm [24]. Around the zero-field-ionization limit, field-induced resonances were only observed in H_2 molecules in 3 kV/cm, but the assignments of the resonances remain incomplete [25]. No experiment has been reported for the field-induced resonances above the zero-field-ionization limit of any core states.

From these examples, it is proper to limit this discussion to diatomic molecules. In their low excited states, the orbital angular momentum of electrons, $\boldsymbol{l}$, is coupled to the internuclear axis by an electric field along the axis, i.e., the "intramolecular field." This is known as Hund's coupling case (a) or (b) (see Fig. 2). In high Rydberg states, where the

*Present address: Photon Factory, Institute of Material Structure Science, KEK, Oho 1-1, Tsukuba, Ibaraki 305-0801, Japan.

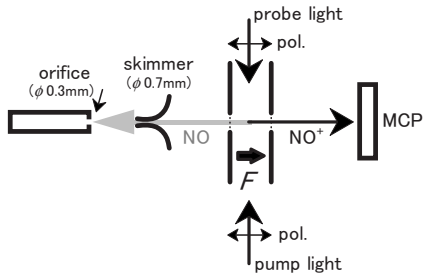

FIG. 1. Schematic view of the experimental setup.

effects from the intramolecular field are weaker, $\boldsymbol{l}$ is coupled to the rotational axis of the core. This is known as Hund's coupling case (d). In a high electric field, it is expected that these changes in the coupling scheme also depend on the strength of the external field relative to the intramolecular field. This competition is not seen in atoms where the external field competes only with the Coulomb binding field. The energy structures of the field-induced resonances reflects these coupling schemes, and their intensity distribution reflects the autoionization dynamics. Dissociation is another molecule-specific aspect of interest. Its dynamics is also expected to be affected by the electric field. It would be exciting to observe the competition between dissociation and field-induced autoionization although the experiment requires additional labor, i.e., species analysis of the fragments. In spite of much interests described above, little is known about the field-induced resonances of high Rydberg molecules because of the above-mentioned experimental difficulty.

In the present study, to overcome the experimental difficulty, (i) nitric oxide (NO) molecules are used because their electronic configuration in the ground state is $(1\sigma)^2(2\sigma)^2(3\sigma)^2(4\sigma)^2(5\sigma)^2(1\pi)^4(2\pi)^1$ $X\,^2\Pi$; thus, they can be considered as one-electron molecules for their high Rydberg states converging to the closed shell $NO^+X\,^1\Sigma^+$ ions, and therefore, their simple energy structures have been studied well. (ii) The double-resonance excitation technique is applied. Then, high Rydberg molecules of a single and lowest vibrational and rotational core state are produced. Their energy structures are as simple as those of the alkali-metal atoms. They are free of the vibrational autoionization or the rotational autoionization. Observation of the field-induced resonances just below and above the zero-field-ionization limit in a high electric field is attempted.

II. EXPERIMENT

Figure 1 shows a schematic view of the experimental setup. In a vacuum chamber, a constant electric field (0–6.67 kV/cm) was generated between a pair of plates spaced 1.2 cm apart and having openings of 30 mm diameter covered with high-transmission (>90%) stainless steel mesh. The deviation of the field from uniformity was estimated to be less than 1%. A pulsed supersonic beam of NO molecules with 180 μs pulse duration, 10 Hz repetition rate, and 3 atm stagnation pressure was generated by an orifice of 300 μm diameter and a conical skimmer of 700 μm diameter. The beam passed through the center of the mesh and went into the field.

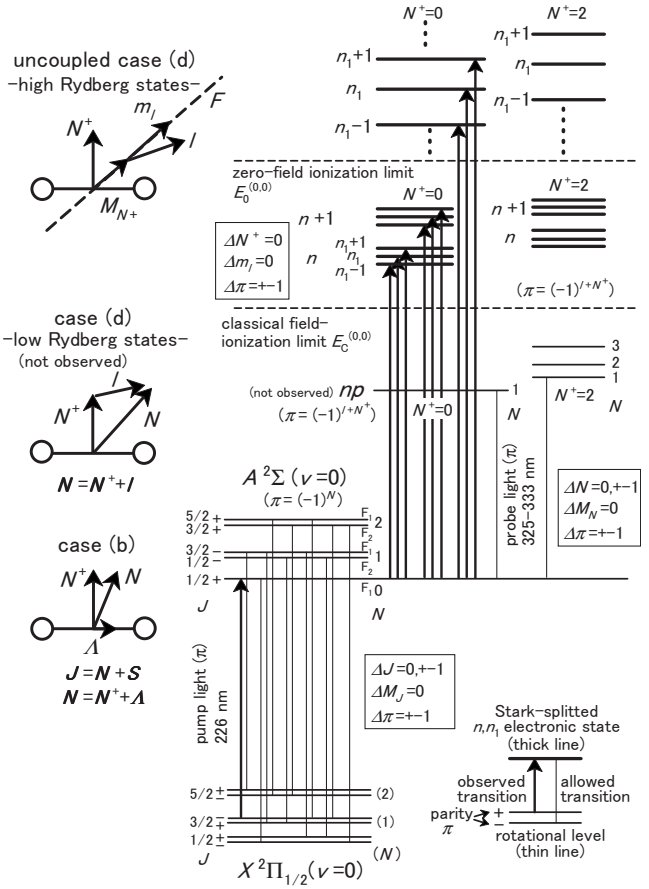

FIG. 2. Schematic energy diagram of NO molecules in an electric field. The successive thin horizontal lines represent the rotational levels denoted by the quantum number N or J for the ground $X\,^2\Pi_{1/2}$ state, the intermediate $A\,^2\Sigma^+$ state, and the low Rydberg np states. For the high Rydberg states, the thick lines represent the Stark-split n and n_1 electronic states belonging to each rotational core state denoted by the quantum number N^+. Above the zero-field-ionization limit $E_0^{(0,0)}$, only n_1 is a good quantum number. Parity π of the level is represented by a symbol + or −. It is given by $\pi=(-1)^N$ for the $A\,^2\Sigma^+F_1(v,N)$ level and by $\pi=(-1)^{l+N^+}$ for the Rydberg level. Allowed transitions are shown by vertical lines, and transitions observed in the present experiment are shown by arrows. Only $\Delta N^+=0$ transitions are observed for the transitions to the high Rydberg n and n_1 states. Coupling schemes of the angular momentum corresponding to each state are also shown.

Figure 2 shows a schematic energy diagram of NO molecules. Pump light (wavelength: 226 nm, bandwidth: 0.18 cm^{-1}, pulse duration: 20 ns, pulse energy: 0.5 mJ/pulse) was generated by frequency-doubling Coumarin 440 dye laser radiation in a beta-barium borate (BBO) crystal. It intersected the molecular beam at right angles in the field. It was linearly polarized parallel to the field. The light excited the NO molecules from the ground $X\,^2\Pi_{1/2}(v=0,J=3/2)$ level to the intermediate $A\,^2\Sigma^+F_1(v=0,N=0,[J=1/2])$ level, where v denotes the vibrational quantum number, and J and N denote the quantum numbers associated with the total angular momentum and the total angular momentum excluding

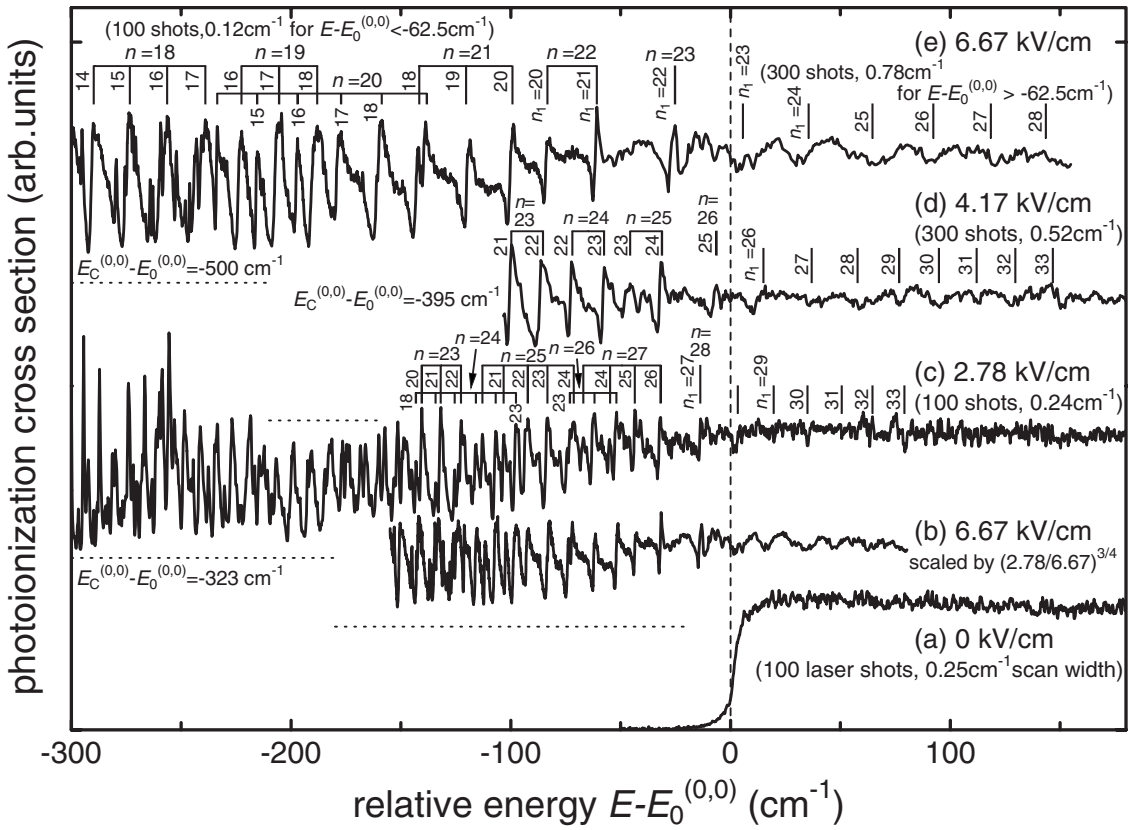

FIG. 3. Photoionization cross section from the $A\ ^2\Sigma^+F_1(v=0,N=0)$ level in arbitral units. The abscissa is the relative energy to the zero-field-ionization limit $E_0^{(0,0)}$(=74 721.7 cm^{-1}). The horizontal broken lines represent the zero positions of the ordinate. Assignments are indicated by the principal quantum numbers n (written horizontally) and the parabolic quantum numbers n_1 (written vertically). The number of the laser shots spent to integrate the ion current and the scan width are shown in parentheses for each cross section. Both are changed at −62.5 cm^{-1} for the cross section at 6.67 kV/cm. For (b), the relative energy $E-E_0^{(0,0)}$ of the cross section is multiplied by $(2.78/6.67)^{3/4}$.

the spin of the electron, respectively. The $A\ ^2\Sigma^+$ state is represented well by Hund's coupling case (b) but is a Rydberg state whose orbital is an almost pure $3s$ orbital by more than 90% [26,27]. No energy shift, no line splitting or no line broadening was observed in the $X\ ^2\Pi-A\ ^2\Sigma^+$ rotational transition lines in the electric field. Therefore, the field-induced rotational level mixing was negligibly small for both the $X\ ^2\Pi_{1/2}$ state and the $A\ ^2\Sigma^+$ state. This is reasonable because the $X\ ^2\Pi_{1/2}$ state and the $A\ ^2\Sigma^+$ state have no neighboring electronic state coupled with them in a field, which is necessary for the Stark mixing between the rotational levels. Probe light (wavelength: 325–333 nm, bandwidth: 0.18 cm^{-1}, pulse duration: 20 ns, pulse energy: 0.5 mJ/pulse) was generated by frequency-doubling 4–dicyanomethylene-2-methyl-6-4-dimethylaminostryl-4H-pyran (DCM) dye laser radiation in a potassium-dihydrogen-phosphate (KDP) crystal. It propagated coaxial and antiparallel to the pump light, polarized parallel to the field, and intersected the molecular beam. It further excited the NO $^2\Sigma^+F_1(v=0,N=0)$ molecules 250 ns after the pump excitation by the double-resonance technique to the energy region around the zero-field-ionization limit $E_0^{(0,0)}$(=74721.7 cm^{-1}) to $NO^+X\ ^1\Sigma^+(v^+=0,N^+=0)$ ions, where "+" on the quantum numbers indicates that they are associated with NO$^+$ ions (core of NO molecules). Only $v=0$ molecules or $v^+=0$ ions were produced due to the Frank-Condon principle.

NO$^+$ ions produced through field-induced autoionization or through direct ionization were accelerated by the same electric field and detected by a microchannel plate. By a gated time window, a boxcar integrator excluded ion current produced by two-photon absorption of the pump light and integrated all current produced by the two-color absorption. The integrated current was recorded simultaneously along with the pulse energy of both laser beams and normalized by the latter. This procedure is named "procedure I." For measurement in a zero-field pump and probe light irradiated the molecules simultaneously with the pulse energy of the pump light reduced to suppress ion current from two-photon ionization to a negligible level. By applying a pulsed electric field of 1.39 kV/cm and 100 μs duration 1 μs after the laser excitation, ion current was recorded. This procedure is named "procedure II." For both procedures, considerable attention was paid to the stability of the experimental conditions, such as the pulse energy of the laser light, the molecular-beam density, and the efficiency of the detector.

III. RESULTS AND DISCUSSION

Figure 3(a) shows the result where the ion current, which is proportional to the photoionization cross section, was measured as a function of the frequency of the probe light at zero

electric field strength according to procedure II. The photoionization cross section is negligibly small below $E_0^{(0,0)}$ and nearly constant above $E_0^{(0,0)}$. In a constant electric field of 2.27, 4.17, and 6.67 kV/cm, procedure I was carried out. Results are shown in Figs. 3(c)–3(e). The cross section is negligibly small below the classical field-ionization limit $E_C^{(0,0)}$ to the $NO^+X\ ^1\Sigma^+(v^+=0,N^+=0)$ ions, which is beyond the lower-energy limit of the figure. Above $E_C^{(0,0)}$ up to $E_0^{(0,0)}$, it contains a series of asymmetrical resonance structures originating from field-induced autoionization. The relative energy $E-E_0^{(v^+,N^+)}$ of the resonances belonging to the series converging to the $NO^+X\ ^1\Sigma^+(v^+,N^+)$ ion scales with $F^{3/4}$ in the vicinity of $E-E_0^{(v^+,N^+)}=0$, where $E_0^{(v^+,N^+)}$ is the zero-field-ionization limit to the $NO^+X\ ^1\Sigma^+(v^+,N^+)$ ions [3,13]. Figure 3(b) shows the cross section at 6.67 kV/cm, where its relative energy $E-E_0^{(0,0)}$ is multiplied by $(2.78/6.67)^{3/4}$. In the vicinity of $E_0^{(0,0)}$, the number of resonance structures contained in this cross section and their energy are in complete agreement with those at 2.78 kV/cm shown in Fig. 3(c). Therefore, the core state of all these resonances is the same $NO^+X\ ^1\Sigma^+(v^+=0,N^+=0)$ state. Here, it should be noted that the following three facts have been also taken into consideration to derive the above conclusion. (i) The energy shifts of the vibrational levels and the N-rotational levels of the intermediate $A\ ^2\Sigma^+$ state are already confirmed to be negligibly small in a field. (ii) The energy spacings among the vibrational levels of the core ($NO^+X\ ^1\Sigma^+$) of the high Rydberg states are independent of F. (iii) The energy spacings among the N^+-rotational levels of the core of the high Rydberg states is possible to depend on F if the field-induced mixing occurs in the N^+-rotational levels. However, their energy shifts do not scale with $F^{3/4}$. The above conclusion is also confirmed by the fact that the cross section has only one threshold energy which coincides with $E_0^{(0,0)}$ at zero electric field strength and with $E_C^{(0,0)}$ (beyond the limit of the figure) in a field. It is summarized that the field-induced mixing among the N^+-rotational levels of the core is negligible. This is reasonable because the core $NO^+X\ ^1\Sigma^+$ state has no neighboring electronic state coupled with it in an electric field.

Resonances that belong to the $NO^+X\ ^1\Sigma^+(v^+=0,N^+=0)$ core state *just below* $E_0^{(0,0)}$ are assigned according to the assumption that $\boldsymbol{l}$ is decoupled from $\boldsymbol{N}^+$ and quantized along the field. Originally this coupling form had been proposed for molecules in a high magnetic field and was called "uncoupled case (d)" [28,29]. In this case, since the Rydberg electron behaves as in an alkali-metal atom, the electronic state of the n-manifold splits into hydrogenic Stark levels represented by the same quantum numbers n, n_1, n_2, and m_l as those of an alkali-metal atom, and a similar field-induced autoionization occurs. Here, the intramolecular field also contributes to the core coupling, in addition to the non-Coulomb part of the core potential. In the vicinity of $E_0^{(0,0)}$, the energy E of the hydrogenic Stark levels cannot be calculated correctly even by fourth-order perturbation theory. Here, it is calculated by using the Bohr-Sommerfeld quantization condition with WKB correction for ξ component [12,13],

$$\int_{\xi_i}^{\xi_o}\sqrt{\frac{E-E_0^{(0,0)}}{2}+\frac{Z_1}{\xi}-\frac{m_l^2}{4\xi^2}-\frac{F\xi}{4}}\,d\xi=\left(n_1+\frac{1}{2}\right)\pi, \quad (1)$$

where Z_1 is the effective charge binding the electron in the ξ coordinate [1,2], and ξ_i and ξ_o are the inner and the outer classical turning points, respectively.

All the well-resolved resonances just below $E_0^{(0,0)}$ are completely attributed to the $m_l=0$ components of the hydrogenic Stark levels. In Fig. 3, assignments are represented by n and n_1. The field-induced resonances in the vicinity of the zero-field-ionization limit $E_0^{(0,0)}$ are completely assigned. Fano profiles induced by the interference in the transition to the discrete high n_1 Stark level and the low n_1 continuum are observed as clearly as in atoms. These successful results are obtained because overlapping of resonances belonging to different core rotational states is absent. The successful assignment confirms the decoupling of $\boldsymbol{l}$ from $\boldsymbol{N}^+$, which has been introduced as an assumption. As a result of the decoupling, it is reasonable that the state of the core remains unchanged ($\Delta N^+=0$) during the electronic transition. The appearance of only the $m_l=0$ component is appropriate because the $A\ ^2\Sigma^+$ state has a nearly pure atomic s-character [26,27]. It is concluded that for an external electric field strength in the range of kV/cm, molecular characteristics are lost in the energy structures just below the zero-field-ionization limit $E_0^{(0,0)}$.

For low Rydberg states where the intramolecular field is dominant, the coupling $\boldsymbol{N}=\boldsymbol{l}+\boldsymbol{N}^+$ holds well. If these states are probed, the $M_N=0$ component (projection of $\boldsymbol{N}$ along the quantization axis) of $N=1$ levels formed from a $np(l=1)$ electronic state and $N^+=0,2$ cores would be excited in a zero field by the selection rules; $\Delta N=0,\ \pm 1$, $\Delta M_N=0$, $\Delta\pi=\pm 1$ [30], where π is the parity of the level represented by $\pi=(-1)^N$ for the $A\ ^2\Sigma^+$ state and by $\pi=(-1)^{l+N^+}$ for the Rydberg states (Fig. 2). In an electric field, the field-induced mixing between N levels would make the energy structures far more complicated.

In the present study, the vibrational state and the rotational state of the core are limited to a single state by applying the double-resonance technique through a properly selected intermediate level of an appropriate molecular species. Furthermore, the decoupling of $\boldsymbol{l}$ and $\boldsymbol{N}^+$ simplifies the energic structure of the molecular resonances to become identical to that of an atom. These allow a complete identification of the observed molecular resonance structure.

Many experiments have proved that the lifetimes of the high Rydberg states of NO molecules are determined by predissociation [31,32]. Thus, their decay rates depend on the orbital angular momentum $\boldsymbol{l}$ of the Rydberg electron. The rates are listed in Ref. [33], where the rate of the p state is the highest and that of the high-l ($l>3$) states is the lowest. From these rates, the lifetimes of the $n=20$–100 Rydberg states are estimated to be several hundred picoseconds for the p states and ~ 100 ns for the high-l ($l>3$) states. In the zero-field case of the present experiment, the high Rydberg states have a strong atomic p-character because of the nearly pure atomic s-character of the intermediate $A\ ^2\Sigma^+$ state. Thus, these high Rydberg molecules decay into neutral atoms through the predissociation long before the pulsed field is

applied that is 1 μs after the photoexcitation, and no ion current is detected for $E<E_0^{(0,0)}$ in Fig. 3(a). Its weak tail just below $E_0^{(0,0)}$ might be caused by the long-lived high-l ($l>3$) Rydberg molecules of $n>100$ excited from the $A\ ^2\Sigma^+$ state through its slight high-l character because the lifetimes of these high Rydberg states are estimated to be longer than 1 μs. In a constant electric field, the predissociation rates of the $n=20-100$ Rydberg states are estimated to be less than their zero-field values that are (several hundred picoseconds$\times 2\pi)^{-1}$ because the long-lived high-l character is mixed into these states. From the observed resonance widths, the lifetimes of the field-induced resonances in Figs. 3(c)–3(e) are determined to be ~ 1 ps. Therefore, the field-induced autoionization process is the dominant decay process rather than the predissociation in the range of the electric field strength in the present experiment.

Above the zero-field ionization limit $E_0^{(0,0)}$, broad resonances are clearly observed at 6.67 kV/cm. A long integration time corresponding to 300 laser shots is necessary to record them with such a good signal-to-noise (S/N) ratio. In the lower field, the S/N ratio of the cross sections degrades, but resonances can be recognized. The field-induced resonances with positive energy are represented by only two good quantum numbers, n_1 and m_l. The Bohr-Sommerfeld quantization condition [Eq. (1)] with $Z_1=1$ gives the lower-energy edge of the resonance and that with $Z_1=0$ gives the higher edge [12,14]. The calculated energy of the lower edge of the $m_l=0$ component is shown by a vertical bar in Fig. 3. It is understood that the calculated energy spacings show well the $F^{3/4}$-dependence (dependence on the field strength) in the vicinity of $E_0^{(0,0)}$. At all field strengths, the energy spacing and positions are in good agreement with the experimental results, and thus, the observed resonances are confirmed to be the field-induced resonances with positive energy. The successful assignment by the Bohr-Sommerfeld quantization condition given by Eq. (1) means that also in the positive energy region, the orbital angular momentum of the electron is decoupled from the core rotation. The success in observing the electric-field-induced resonances above the zero-field-ionization limit of molecules is due to the absence of overlapping of resonances belonging to different core states.

The shape of the resonance structure is determined by the product of the density of states and the square of the normalized associated Legendre polynomial $P^2_{lm_l}(2Z_1-1)$, where Z_1 takes values from 0 to 1 varying with E from the higher- to lower-energy edge of the resonance [14]. The function $P^2_{lm_l}(2Z_1-1)$ represents the l-character in the n_1, m_l resonances. Since the density of states is a slowly varying function of energy E, the shape of the resonance structure is mainly determined by the P^2_{10} function, considering that the intermediate $A\ ^2\Sigma^+$ state has a nearly pure atomic s character. Thus, the shape resembles that of resonances excited from the s state of atoms [8], while resonances excited from the p state [10,12] have steep lower-energy edges due to the d-character (P^2_{20}) in the resonance.

Figure 4 shows classical trajectory calculations. In Fig. 4(a), a positive charge $+e$ is placed at the origin and an electric field of 6.67 kV/cm is applied in the positive z direction. This represents the core of an atom in an electric field. The broken curve shows the trajectory where the electron starts at rest 50.5 nm from the origin and 7 nm from the z axis ($b_0=7$ nm), and thus, its total energy $E-E_0$ is *positive* +43.9 cm^{-1}. The electron is accelerated in the negative z direction by the external field. Approaching the core, it then bends in a highly eccentric orbit passing close to the core and moves off in the positive z direction where it again reverses direction under the influence of the external field. The electron repeats this cycle of motion two times and then ionizes. The solid curve shows the trajectory with $b_0=1.5$ nm as initial condition. The cycle repetition increases to three times, which means that the resonance state is more stable when the electron cloud concentrates along the z axis.

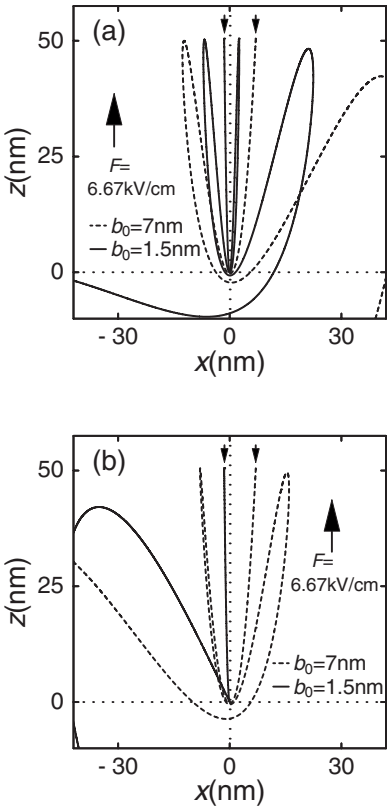

FIG. 4. Classical trajectory calculations. (a) Case of atoms. A positive charge $+e$ is placed at the origin and an electric field of 6.67 kV/cm is applied in the positive z direction. The broken curve shows the trajectory where the electron starts at rest 50.5 nm from the origin and 7 nm from the z axis ($b_0=7$ nm), and thus, its total energy $E-E_0$ is *positive* +43.9 cm^{-1}. The starting position is indicated by a short arrow. The solid curve shows the trajectory with $b_0=1.5$ nm as initial condition. (b) Case of molecules. Two positive charges $+e$ are placed at $(x,z)=(+0.053,0)$ and $(x,z)=(-0.053,0)$ in units of nm, respectively, and a negative charge $-e$ is placed at the origin. The broken curve shows the trajectory with $b_0=7$ nm and $E-E_0^{(0,0)}=+43.9$ cm^{-1} as initial condition. The solid curve shows that with $b_0=1.5$ nm.

In Fig. 4(b), two positive charges $+e$ are placed at $(x,z)=(+0.053,0)$ and $(x,z)=(-0.053,0)$ in units of nm, respectively, and a negative charge $-e$ is placed at the origin. These represent the core of an NO molecule (NO^+), where the valence electron cloud of the NO^+ is approximated to be con-

centrated on the internuclear axis. The broken curve shows the trajectory with $b_0=7$ nm as initial condition. This trajectory is similar to that with the $b_0 \sim 4$ nm condition for atoms. The difference in b_0 that results in the similar trajectory for atoms and molecules is caused by the size difference of the cores. The period of one cycle is calculated to be 1.19 ps, which corresponds to the energy spacing of 28.0 cm^{-1} between resonances. This spacing is in good agreement with the observed spacing of ~ 27 cm^{-1} in the energy region near $E-E_0^{(0,0)}=+43.9$ cm^{-1} at an electric field strength of 6.67 kV/cm [Fig. 3(e)]. Figure 4 explains that these resonances correspond to the transient states of electrons trapped along the z axis on the "uphill" side of the potential energy. It is consistent with the fact that the molecules are excited by the light linearly polarized parallel to the field from the $A\ ^2\Sigma^+$ state that has a nearly pure atomic s-character to these resonances; thus, they have an atomic p and $m_l=0$ character, and therefore, the electron cloud of the molecule is constrained along the z axis. The solid curve shows the trajectory with $b_0=1.5$ nm as initial condition. The trajectory is not quasibound due to the effects from the intramolecular field although the effects are exaggerated by ignoring the core rotation, the spatial distribution, and the recoil of the electrons of the core. It is understood that for atoms, the resonance state becomes more stable as the electron is constrained more *tightly* along the z axis (field direction), but the same is not true for molecules. This might be the reason for the difficulty in observing the electric-field-induced resonances with positive energy in molecules.

ACKNOWLEDGMENTS

This work was partly supported by a Grant-in-Aid for Scientific Research from the Japan Society for the Promotion of Science (JSPS) (Grant No.18540396).

[1] H. A. Bethe and E. E. Salpeter, *Quantum Mechanics of One- and Two-electron Atoms* (Plenum, New York, 1957).
[2] T. F. Gallagher, *Rydberg Atoms* (Cambridge University Press, New York, 1994).
[3] R. R. Freeman and N. P. Economou, Phys. Rev. A **20**, 2356 (1979).
[4] M. G. Littman, M. M. Kash, and D. Kleppner, Phys. Rev. Lett. **41**, 103 (1978).
[5] S. Feneuille, S. Liberman, E. Luc-Koenig, J. Pinard, and A. Taleb, Phys. Rev. A **25**, 2853 (1982).
[6] J. M. Lecomte, S. Liberman, E. Luc-Koenig, J. Pinard, and A. Taleb, Phys. Rev. A **29**, 1929 (1984).
[7] S. Feneuille, S. Liberman, J. Pinard, and A. Taleb, Phys. Rev. Lett. **42**, 1404 (1979).
[8] R. R. Freeman, N. P. Economou, G. C. Bjorklund, and K. T. Lu, Phys. Rev. Lett. **41**, 1463 (1978).
[9] T. S. Luk, L. Di Mauro, T. Bergeman, and H. Metcalf, Phys. Rev. Lett. **47**,83(1981).
[10] W. Sandner, K. A. Safinya, and T. F. Gallagher, Phys. Rev. A **23**, 2448 (1981).
[11] W. L. Glab and M. H. Nayfeh, Phys. Rev. A **31**, 530 (1985).
[12] H. Rottke and K. H. Welge, Phys. Rev. A **33**, 301 (1986).
[13] A. R. P. Rau, J. Phys. B **12**, L193 (1979).
[14] E. Luc-Koenig and A. Bachelier, J. Phys. B **13**, 1743 (1980); J. Phys. B **13**,1769 (1980).
[15] G. Alvarez and H. J. Silverstone, Phys. Rev. Lett. **63**, 1364 (1989).
[16] M. Courtney, H. Jiao, N. Spellmeyer, D. Kleppner, J. Gao, and J. B. Delos, Phys. Rev. Lett. **74**, 1538 (1995).
[17] V. Kondratovich, J. B. Delos, N. Spellmeyer, and D. Kleppner, Phys. Rev. A **62**, 043409 (2000).
[18] D. J. Armstrong, C. H. Greene, R. P. Wood, and J. Cooper, Phys. Rev. Lett. **70**, 2379 (1993).
[19] B. Broers, J. F. Christian, J. H. Hoogenraad, W. J. van der Zande, H. B. van Linden van den Heuvell, and L. D. Noordam, Phys. Rev. Lett. **71**, 344 (1993).
[20] G. M. Lankhuijzen, M. Drabbels, F. Robicheaux, and L. D. Noordam, Phys. Rev. A **57**, 440 (1998).
[21] Ch. Bordas, F. Lépine, C. Nicole, and M. J. J. Vrakking, Phys. Rev. A **68**, 012709 (2003).
[22] J. Chevaleyre, C. Bordas, M. Broyer, and P. Labastie, Phys. Rev. Lett. **57**, 3027 (1986).
[23] W. L. Glab and K. Qin, Phys. Rev. A **48**, 4492 (1993).
[24] J. B. M. Warntjes, F. Robicheaux, J. M. Bakker, and L. D. Noordam, J. Chem. Phys. **111**, 2556 (1999).
[25] W. L. Glab and J. P. Hessler, Phys. Rev. A **42**, 5486 (1990).
[26] S. N. Dixit, D. L. Lynch, V. McKoy, and W. M. Huo, Phys. Rev. A **32**, 1267 (1985).
[27] W. Y. Cheung, W. A. Chupka, S. D. Colson, and D. Gauyacq, J. Chem. Phys. **78**, 3625 (1983).
[28] D. Gauyacq, M. Raoult, and N. Shafizadeh, in *The Role Of Rydberg States In Spectroscopy And Photochemistry*, edited by C. Sándorfy (Kluwer Academic, Dordrecht, 1999) Chap. 13.
[29] T. S. Monteiro and K. T. Taylor, J. Phys. B **22**, L191 (1989).
[30] A. L. Goodgame, H. Dickinson, S. R. Mackenzie, and T. P. Softley, J. Chem. Phys. **116**, 4922 (2002).
[31] M. J. J. Vrakking and Y. T. Lee, Phys. Rev. A **51**, R894 (1995).
[32] M. J. J. Vrakking and Y. T. Lee, J. Chem. Phys. **102**, 8818 (1995).
[33] M. J. J. Vrakking, J. Chem. Phys. **105**, 7336 (1996).